SAND99-2784C

Society of Petroleum Engineers

IADC/SPE 59178

Advanced Transient Simulator for Studying Shallow Gas Blowouts

J.S. Rath, Sandia National Laboratories, and A.L. Podio, University of Texas Austin

This paper was prepared for presentation at the 2000 IADC/SPE Drilling Conference held in New Orleans, Louisiana, 23–25 February 2000.

Abstract

Two wellbore hydraulics simulators (KICK[1] and COMBOF[2,3]) were modified to simulate high flow rate from overpressured high permeability formations in order to study the necessary reaction time to avoid a blowout event. This paper describes the computational approaches and results of calculations using these two different numerical wellbore hydraulic simulators. The coupling of the wellbore and the reservoir model is an important aspect of these simulators. The wellbore is coupled to an overpressured highly permeable zone through the use of an influence function. An influence function is an externally generated linear system whereby a change in pseudo-pressure yields a change in cumulative gas influx (or mass flow rate). This influence function can be generated from a suitable two-phase flow reservoir simulator, prior to the wellbore hydraulic simulator calculations. The KICK numerical simulator uses a moving boundary approach to more accurately describe the multi-phase fluid mixing and transport during drilling activities. Both simulators were used to analyze potential blowout scenarios at the Waste Isolation Pilot Plant (WIPP) transuranic waste (TRUW) repository.

Introduction

The WIPP is a geological repository designed for the permanent disposal of TRUW. The WIPP facility is located in southeastern New Mexico. Disposal regions are approximately 650m below ground surface, and are mined from the bedded salt of the Salado Formation. Regulatory requirements dictate that performance assessment calculations must include the processes and effects of an inadvertent intrusion by a drilling operator. If an exploratory well was drilled into a pressurized geologic TRUW repository, a sudden influx of gas and underground water might occur.

The two different numerical simulators were used to analyze a blowout scenario at the WIPP. The influence function capability was adapted to both numerical models. An extensive study shows that casing pressure and pit gain (or mud volume) response was different using the two simulators with identical initial conditions and material properties. However, the modified KICK numerical model incorporates the correct wellbore fluid dynamics and describes the non-steady state reservoir behavior more accurately. Another finding was that simulated mud volume expulsion profiles were dependent upon several key parameters: permeability of the formation, gas specific gravity, gas slip velocity, rate of penetration, and pumping rate.

Numerical Simulator, KICK: Moving Boundary Technique

Podio[1] developed the moving boundary solutions of mass and momentum balance technique to analyze wellbore hydraulics during common petroleum drilling practices. The KICK model can then be used to simulate drilling into an overpressured permeable region whereby a constant BHP which is sufficiently greater than the formation pressure so as to prevent further influx of formation fluids but not so high as to fracture the formation. A more realistic approach of gas distribution throughout the annulus is approximated using numerous discrete sections with variable gas concentrations. The model also includes the dynamic effects of variable pump rate, formation influx distribution, BOP (blow out preventers), and choke closure. These features allow predictions of detailed flow and pressure response of the well (*i.e.*, bottom hole) at all times and at wellbore locations during a *"gas kick"*. The model uses a moving boundary solution to solve the mass and momentum balance equations and also incorporates proper mathematical treatment of gas influx, slip velocity, and friction factors. Figure 1 shows the wellbore configuration used in the KICK numerical code. The KICK model does not consider any "spalled" material volume entering the wellbore from the drill bit penetrating an over pressured gas zone. It only considers drill cuttings as solid material entering the wellbore and being transported up the annulus, mixed with gas and fluids. However, the transport of the mixture of drill cuttings, gas, and drilling fluids up the annulus is computed using conservation momentum equations and mass balances.

Thus, the KICK model will not add any more solid material other than drill cuttings to be transported up the annulus when drilling rates (*i.e.,* rate of penetration) have stopped. Because of this, only drilling mud (if mud-pumping operations are still on) and gas are allowed to enter the wellbore and be transported up the annulus. The absence of a "spalled" solid material entering the wellbore is another difficulty in directly comparing the two numerical simulators. The schematic of the KICK conceptual model of drilling operations is shown Figure 2. Figure 2 displays the drilling mud entering the top of the drilling rig (inner pipe) at the left end and flowing down (due to pumping operations) to the bottom hole. At bottom hole, the drill bit may be off-bottom (a KICK control parameter) and then mud, drill cuttings, and geologic fluid are flowing up the annulus, as shown on the right side of Figure 2.

Modifications to Original KICK Code. To compare calculations, the influence function capability was adapted to the KICK numerical model. This was accomplished through a geometric factor related to depth of drill bit penetration into the pressurized TRUW repository. An alternative interpretation of "influence function" [see Appendix A] was added to the KICK code to correctly handle the amount of added gas (volume) entering the annulus. This was accomplished by using the length of gas zone exposed to the wellbore (or drill bit contact length with the gas zone) combined with the output information from the influence function.

Numerical Simulator, COMOBF: Single Slug Velocity Technique

Mishra, *et al.*[3] developed the single slug velocity method used in the COMBOF code. The numerical model uses a pressure differential approach, whereby a drilling process bottom hole pressure (BHP) intersects a highly pressured region representing the TRUW repository. It also simulates the physical processes of mud and gas transport up the drill string annulus, solids transport within the gas phase, and hydraulic coupling of the intrusion borehole with the TRUW repository. COMBOF dynamically handles "single slug" movement of both mud, and the gas-and-solids mixture up the annulus as shown in Figure 3. However, COMBOF does not allow any mixing of the influx gas with the mud and always maintains a mud and gas interface (which also contains solids) until all the mud has been expelled. The unique feature of the COMBOF numerical model is the coupling of pressurized repository response through the use of an influence. The influence function used in all analyses was generated by TOUGH28W[4] calculations assuming a penetration depth of 0.01m into a WIPP waste panel and a terminal gas wellbore pressure of 8.0 MPa. Figure 4 displays the cumulative gas production from TOUGH28W calculations for two different WIPP waste panel penetration depths. A schematic of the linear system of the Influence function is shown as Figure 5. Figures 6 and 7 depict the Influence function vs. time and the pseudo-pressure vs. pressure used for all wellbore hydraulics simulator calculations.

The COMBOF model uses a temperature-dependent gas viscosity function. The dependent viscosity terms are also used in the computation of friction factors. Both viscosity and friction factors are critical components for calculating the pressure drop. The pressure drop equations are a result of momentum balances for both the single slug "mud" region and the single slug "solids and gas" region movement along (or vertically up) the annulus.

The COMBOF model assumes that the drill bit has stopped at a "penetration depth" which is associated with the externally derived (*i.e.*, two-phase flow reservoir simulator [TOUGH28W version 2.0][5]) influence function from which the gas influx is determined. The mechanism for adding solid materials into the wellbore (bottom of well) is accomplished by limiting the solids-to-gas volume flow ratio, which is an input parameter (In ref. 4, the COMBOF calculations limited the allowable solids/gas to 4%). To accommodate transport of "spalled" material inside the annulus mixed with gas, first the mass of solid material entering the wellbore is estimated. A solid material flow rate is determined from either the available "spalled" material volume or the gas flow rate. The available spalled material volume is an input parameter, and the gas flow rate is determined from the influence function. The solid material flow rate (units of volume/time) entering the wellbore is taken as the smaller quantity of either: (1) the available spalled material volume divided by the time step or, (2) the maximum allowable solids/gas volume flow ratio times the gas influx rate (a gas flow rate of volume per time). The spalled solid material mass is computed (specific gravity of 2.65 was used in all calculations) and that mass is then subtracted from the available spalled material mass, setting up for the next calculation time step, etc. It is then assumed that the wellbore contains a mixture of gas and solids that are to be transported up the annulus of the drill string. Since no drilling operations are assumed, there is no downward movement of the drill bit and/or any additional drilling mud (or fluids) added to the transported mixture of solids and gas traveling up the annulus (related to real drilling pumping rates, etc.). Thus, this portion of the COMBOF model considers a "slug" containing a mixture of gas and solids following behind the other "slug" of drilling mud within the annulus which is traveling upward. After all the mud has been ejected (blowout scenario), the pressure boundary conditions are adjusted (pressure at the top of the annulus is forced to be atmospheric) and only the mixture of gas and solids remains in the annulus. There is no contribution from the inner drill string (containing the drilling mud in a real drilling operation) to the wellbore and/or gas influx. The COMBOF model does not consider any solids from cuttings, entering the solids and gas region because of the assumption and initial position of the drill bit penetration into the pressurized repository region. At time=0 the drill bit is assumed to have penetrated the repository a distance of 0.01m (ref. 3). Previous analyses had coupled the COMBO code with a two-phase flow code (TOUGH28W) to generate an influence function. [The influence function is dependent on the terminal bottom hole pressure (BHP) condition, waste region permeability, and drill bit penetration

DISCLAIMER

depth.]. The influence function is the driving force for gas influx and an assumed "spalled" material (solids) rate, which enters the wellbore and is transported as a mixture of solids and gas up the annulus. This model neglects the drilling mud (which would be pumped down the inner pipe) entering the wellbore during real drilling operations. This neglect of a liquid phase entering the wellbore is one source of difficulty in comparing the two numerical models.

Results

Two sets of sensitivity calculations, using each transient simulator show how various input parameters influence the mud volume expulsion that might occur during a "gas kick" event. A schematic of the drilling rig dimensions used in all wellbore hydraulics calculations is given as Figure 8 (modified from ref. 5)

Case studies 1 and 2 are sensitivity analyses using the numerical simulators, COMBOF and KICK. Case study 3 investigates shallow gas blowout scenarios, were the influence function was used and incorporates added "spalled" solid material entering the wellbore during penetration into the gas zone. Three physical phases of material are transported up the annulus and simulated in the KICK code as the gas-liquid-solids mixture. Case study 3 involves the KICK numerical simulator exclusively.

Case Study 1. A small-scale sensitivity analysis was performed to observe the trends influencing the gas-mud interface (GMI) elevation response using the COMBOF code. Three different input parameters were varied to observe the overall effect on GMI elevation response: Drilling mud density, maximum allowed solids-to-gas volume flow ratio, and drilling mud viscosity. The base-case input parameter values are listed in Table 1 and the three other input parameter value ranges are specified in Tables 2-4. The corresponding GMI elevation response histories of these three sensitivity calculations are shown in Figures 9-11. As expected, as drilling mud density was increased the time of GMI reaching the surface elevation was increased (Fig. 9), and a similar trend was found when the maximum allowed solids-to-gas volumetric flow ratio increased (Fig. 11). The effect of varying the drilling mud viscosity over two orders of magnitude did not significantly change the time of GMI reaching the surface elevation (Fig. 10). Comparing Figs. 9 and 11, (drilling mud density 980.0 to 1277.5 kg/m^3, and max. allowable solids to gas volumetric ratio 1 to 6%) reveals drilling mud density and the mixture composition are sensitive parameters related to blowout times.

Case Study 2. This sensitivity study was performed using the KICK code and varied drilling operation parameters. Three KICK input parameters (not related to drilling rate, or rate of penetration [ROP]) were varied to demonstrate geologic and material properties related to the drilling environment affect the GMI elevation response: drilling mud density, gas slip velocity, and permeability of the "gas zone" or repository region. These sensitivity calculations were completed using the original "steady drainage radius" (ref. 1) gas influx function without the influence function method of gas influx method. Shown in Table 5 is the drilling sequence used in all KICK sensitivity calculations. The KICK code requires a "stabilization time", t_{stab}, for drilling simulations before penetration rates, mud pumping rates, etc. can be started. A value of t_{stab}=2 minutes was used for all KICK calculations. The time that the wellbore is exposed to the gas zone as the drill bit penetrates into the gas zone is a function of the ROP. For all KICK sensitivity calculations the product of gas zone exposed time and length of wellbore exposed to the gas zone was 810 inch-seconds. Tables 6 through 9 display the base-case input parameter values and the three sensitive input parameter values used during the KICK sensitivity calculations. The corresponding GMI elevation response histories of these three sensitivity calculations are shown in Figures 12–14. As seen in Figure 14, the permeability has a great impact on the GMI elevation response. The other parameters (gas slip velocity and drilling mud density) had a small influence on the time of the GMI to reach the surface elevation. When the drilling mud density was increased (Fig. 12) the time for the GMI to reach the surface elevation increased and is in agreement with the COMBOF drilling mud density sensitivity calculation (compare with Fig. 9). Varying the gas slip velocity (and using a gas slip velocity of 0.0) has a small effect on the time of GMI to reach the surface elevation (Fig. 13).

Case Study 3. In order to investigate the "spalling" effect (introduction of a failed solid-phase material volume into the wellbore) an enhancement was made to the KICK code. This modification allowed solid-phase material to flow (with the gas) into the wellbore exactly the same way that COMBOF incorporated solid material flowing into the "solids-gas" region. However, using the KICK numerical model, now all three phases are present in the wellbore (if the drill mud-pumping rate is non-zero). Incorporating spalling, all three phases are available for transport using the momentum balance equations and moving boundary method inherent to the KICK numerical model. Two additional input parameters were needed for this option (to incorporate spalling effects): the maximum allowed solids-to-gas volume flow ratio, and the available solid-phase material volume. These two variables are identical to the input parameters used in the COMBOF model. Since the KICK model already handles solid-phase material volume entering the wellbore, as drill cuttings, the additional solid-phase material volume contribution and corresponding reduction in gas volume was readily adapted into the numerical model.

Several KICK calculations were completed using various solids-to-gas volume flow ratios to determine if the flow up the annulus could be "choked". This "choked" behavior occurs when the flow of drilling mud (liquid phase) plus gas (gas phase) plus spalled solid material (solid phase) flowing together as a mixture up the annulus is severely slowed and/or even becomes stalled. Table 10 shows the range of the Solids-to-Gas volume flow ratios used in the "added spalling" KICK calculations. Figures 15 through 16 show the GMI response and the gas influx rate history for all the solids-to-gas volume flow ratios used, as well as the base case with and without the

influence function. As seen in the Figures 15 and 16 the increased solids-to-gas volume flow ratio substantially reduces the available gas entering the wellbore. In addition this increasing of the solids-to-gas volume flow ratio (i.e., controlling the amount of spalled solid-phase material volume entering the wellbore) has a large impact on response time for the GMI history – it retards the GMI time to reach the surface elevation. Thus the increased spalled solid-phase volume entering the wellbore reduces the gas volume (which reduces the amount of volume available for compression) and has the effect of increasing the wellbore pressure acting on the fluid mixture (solids, liquids, and gas) traveling up the annulus. This decrease in gas volume (and increase in solids volume) alters both the conservation of mass and momentum balance equations of KICK model which solve the displacement, velocity, and acceleration of the mixture (now containing all three phases) traveling up the annulus. The overall effect is a decreased mixture velocity, which slows the response for all mixture components traveling up the annulus. As seen in Figure 15 the arrival time of the GMI to the surface elevation decreases when more solid-phase material volume (i.e., spalled material) is added to the wellbore. The modified KICK numerical model encountered numerical problems (related to lost circulation) when the solids-to-gas volume flow ratio exceeded 10% (spalled solid-phase material volume = 10% gas phase volume entering the wellbore). This numerical problem suggests that some type of "choking" was encountered and that the 10% solids-to-gas volume flow ratio is a rough value for the limitation of this enhancement to the KICK model.

Figure 17 shows the pit gain (mud volume) affected by increased spalling mechanism. Similar to the trend of Figure 15, as more spallings is allowed to be included as solid phase, the pit gain is occurs faster.

Conclusions

1. The modified KICK code is capable of accurate simulation of kick conditions in highly permeable sands since it describes correctly the transient phenomena and the entrainement of solids into the flow stream thus allowing the possibility of stuyding the flow choking effect leading to wellbore bridging.
2. Influence functions can greatly simplify shallow gas blowout calculation.
3. Modified KICK numerical model (with spalling mechanism and Influence function) allows a wide range of drilling operation parameters to be varied to study the time of arrival of a "show" (GMI reaching the surface elevation).
4. The KICK sensitivity study of permeability is inconsistent with the Influence Function. To more accurately predict this effect, the Influence Function should be generated from external reservoir model simulations (i.e., using TOUGH28W) with identical permeabilities.

Nomenclature

BHP = Bottom Hole Pressure
BOP = Blowout Preventers
DBD = Drill Bit Depth
DOE = (United States) Department of Energy
ECD = Equivalent Circulating Density
GMI = Gas-Mud Interface
GZ = Gas Zone
IF = Influence Function
IFGIM = Influence Function Gas Influx Method
ROP = Rate of Penetration
SGVFR = Solids to Gas Volume Flow Ratio
TRUW = Transuranic Waste
WIPP = Waste Isolation Pilot Plant
∇ = gradient operator
$\nabla\cdot$ = divergence
∇^2 = Laplacian operator
A = area, m [L]
$c_0(p)$ = real gas compressibility defined in equation (A-8), Pa^{-1} [Lt/M]
g = gas mass flux or mass rate, kg/s [M/t]
G = cumulative gas mass, kg [M]
k = permeability, m^2 [L^2]
M = molar mass (molecular weight), kg/(kg·mol) [1]
$m(p)$ = pseudo-pressure, Pa/s [M/(Lt^3)]
p = pressure, Pa [M/(Lt)]
q = volumetric flow rate, m^3/s [L^3/t]
r = radius, m [L]
r_b = radius of the reservoir boundary, m [L]
r_D = dimensionless radius or multiple of well bore boundary radius [1]
q = gas volume flux or volume rate, m^3/s [L^3/t]
Q = cumulative volume, m^3 [L^3]
R_u = universal gas constant = 8314 Pa·m^3/(kg·mol·K)
t = time, s [t]
t_D = dimensionless time [1]
t_{stab} = KICK code stabilization period, s [t]
T = temperature, K [T]
v = velocity, m/s [L/t]
v_{gas_slip} = (KICK parameter) gas-slip velocity, m/s [L/t]
x,y,z = direction notation
$z(p)$ = gas deviation factor, pressure dependent at constant temperature
ρ = density, kg/m^3 [M/L^3]
ρ_{mud} = drilling mud density, kg/m^3 [M/L^3]
$\mu(p)$ = real gas dynamic viscosity, pressure dependent at constant temperature, Poise [M/(Lt)]
ϕ = porosity [1]

Acknowledgments

We thank the U.S. Department of Energy for funding J.S. Rath's work in wellbore hydraulics in support of WIPP recertification activities. Great appreciation is also given to Dr. A.L. Podio for his development of the moving boundary technique and physical interpretation of numerical simulations using the KICK code. In addition, we thank INTERA Inc. (now known as Duke Engineering & Services) for providing documentation and theory of the COMBOF code.

References

1. Podio, A.L., and A.P. Yang. 1986. "Well Control Simulator for IBM Personal Computer," IADC/SPE 14737. International Association of Drilling Engineers/Society of Petroleum Engineers (paper presented at the 1986 IADC/SPE Drilling Conference held in Dallas, TX. February 10-12, 1986).
2. Hansen, F.D., M.K. Knowles, T.W. Thompson, M. Gross, J.D. McLennan, and J.F. Schatz. 1997. "Description and Evaluation of a Mechanistically Based Conceptual Model for Spall," SAND97-1369. Sandia National Laboratories: Albuquerque, NM. Chapter 4, Pages 24-35. {COMBOF - A FORTRAN77 Computer Code for Calculating Bottom Hole Pressure for Fluid with Suspended Solids Flow Using an Externally Generated Influence function.}
3. Mishra, S., D. Fryar, M. Reeves, V. Kelley, B. Statham, and R. Reeves. 1997. "Analysis Package for COMBOF." TSL614-1. INTERA Inc.: Austin, TX.
4. Ibid., pp. 5-6
5. Pruess, K. 1991. "TOUGH2 – A General-Purpose Numerical Simulator for Multiphase Fluid and Heat Flow." LBL-29400. Berkeley, CA: Earth Sciences Division, Lawrence Berkeley Laboratory. (Available from the National Technical Information Service [NTIS], Springfield, VA as DE92000755/XAB.)
6. D. M. Stozel, 1996. "Analysis Package for the BRAGFLO Direct Release Calculations (Task 4) of the Performance Assessment Analyses Supporting the Compliance Certification Application," WPO #405020. Figure 4, Page 187. SWCF-A:1.2.07.4.1:PA:QA:Analyses:AP-029: BRAGFLO Direct Release Calculation (Task4).
7. Al-Hussainy, R., Ramey, Jr., H. J. and Crawford, P.B.: "The Flow of Real Gases Through Porous Media," *JPT, Journal of Petroleum Technology*. May 1966, pp. 624-636.
8. Klinkenberg, L. J.: "The Permeability of Porous Media to Liquids and Gases," *Drilling and Production Practices, API* (1941) 200
9. Aronofsky, J. S.: "The Effect of Gas Slip on Unsteady Flow of Gas Through Porous Media," *Jour. Appl. Phys.* (1954) **201**, 149.
10. Aronofsky, J. S. and Ferris, O. D.: "Transient Flow of Non-ideal Gases in Porous Media-One Dimensional Case," *Journal of Applied Physics* (1954) **25**, 289.
11. van Everdingen, A. F. and Hurst, W.: "The Application of the Laplace Transformation to Flow Problems in Reservoirs," *Trans.*, AIME (1949) **186**, 305.

Appendix-A Influence Functions

The "pseudo-pressure" concept (Al-Hussainy et. al., 1966) can be used to linearize the equations describing transient, single-phase gas flow from the formation to the wellbore. Beginning with the principle of conservation of mass for isothermal fluid flow through a porous media, a continuity equation can be written as

$$\nabla \cdot \left(\rho \underset{\sim}{v}\right) = -\phi \frac{\partial \rho}{\partial t} \quad \text{.....(A-1)}$$

where $\nabla \cdot$, ρ, v, and $\partial/\partial t$ are the divergence operator, gas density, gas velocity, porosity, and partial derivative with respect to time, respectively Assuming that the fluid flow is laminar, and Darcy's law is valid, the velocity vector of equation (A-1) can be written as

$$\underset{\sim}{v} = -\frac{k(p)}{\mu(p)} \nabla p \cdot \quad \text{.....(A-2)}$$

where $\mu(p)$ is the pressure dependent viscosity. Substitution of equation (A-2) into (A-1) yields

$$\nabla \cdot \left[\rho \frac{k(p)}{\mu(p)} \nabla p \right] = \phi \frac{\partial \rho}{\partial t} \quad \text{.....(A-3)}$$

For real gases, the density, ρ, in equation (A-3) can be written as

$$\rho = \frac{M}{R_u T} \left[\frac{p}{z(p)} \right] \quad \text{.....(A-4)}$$

In equation (A-4), M, R_u, and T are the molar mass, universal gas constant, and temperature, respectively. The fraction $\frac{p}{z(p)}$ incorporates real behavior of gas through the use of a gas deviation factor, $z(p)$. Substitution of equation of (A-4) into (A-3) eliminates the density:

$$\nabla \cdot \left[\frac{k(p)}{\mu(p) z(p)} p \nabla p \right] = \phi \frac{\partial}{\partial t} \left[\frac{p}{z(p)} \right] \quad \text{.....(A-5)}$$

By neglecting inverse pressure-dependence on permeability [Klinkenberg, 1941], assuming that variations of other properties associated with gas reservoirs are more important than variations in permeability with pressure [Aronofsky and Ferris, 1954], and assuming that liquid permeability can be used for gas flow, then equation (A-5) can be simplified to the form

$$\nabla \cdot \left[\frac{p}{\mu(p) z(p)} \nabla p \right] = \frac{\phi}{k} \frac{\partial}{\partial t} \left[\frac{p}{z(p)} \right] \quad \text{.....(A-6)}$$

Knowing the form of the isothermal compressibility equation, the partial derivative with respect to time on the right hand side of equation (A-6) can be reduced to

$$\frac{\partial}{\partial t}\left[\frac{p}{z(p)}\right]=\frac{pc_0(p)}{z(p)}\frac{\partial p}{\partial t} \quad \text{.....(A-7)}$$

where the isothermal compressibility function, $c_0(p)$, is defined as

$$c_0(p)=\frac{1}{\rho}\frac{d\rho}{dp}=\frac{z(p)}{p}\frac{d}{dp}\left(\frac{p}{z(p)}\right)=\frac{1}{p}-\frac{1}{z(p)}\frac{dz(p)}{dp} \quad \text{.....(A-8)}$$

Assuming that the dynamic viscosity, $\mu(p)$, and real gas deviation factor, $z(p)$, change slowly with pressure change, or assuming that pressure gradients are small will permit omission of terms of order $(\nabla p^2)^2$, it is found [Al-Hussainy, *et. al.*, 1966] that equation (A-6) can be reduced to the form

$$\nabla^2 p^2=\frac{\phi\mu(p)c_0(p)}{k}\frac{\partial p^2}{\partial t} \quad \text{.....(A-9)}$$

Equation (A-9) is a partial differential equation (PDE) describing non-linear gas flow assuming pressure gradients are small everywhere in the flow system [Al-Hussainy, *et. al.*, 1966]. However by carefully selecting a scale change, equation (A-5) can be transformed to a similar form of equation (A-7) **without the assumption of small pressure gradients** [Al-Hussainy, *et. al.*, 1966]. This transformation begins by defining a pseudo-pressure, $m(p)$, or

$$m(p)=2\cdot\int_0^p\frac{p'}{\mu(p')z(p')}dp' \quad \text{.....(A-10)}$$

It should be noted that the units of pseudo-pressure are pressure-squared per unit dynamic viscosity (*i.e.*, ML/t or Pressure per time). The partial derivative of pseudo-pressure with respect to time, and the gradient of the pseudo-pressure can be found as

$$\frac{\partial}{\partial t}[m(p)]=\frac{\partial[m(p)]}{\partial p}\cdot\frac{\partial p}{\partial t}=\left[\frac{2p}{\mu(p)z(p)}\right]\frac{\partial p}{\partial t} \quad \text{..(A-11)}$$

$$\frac{\partial}{\partial x}[m(p)]=\frac{\partial[m(p)]}{\partial p}\cdot\frac{\partial p}{\partial x}=\left[\frac{2p}{\mu(p)z(p)}\right]\frac{\partial p}{\partial x} \quad \text{..(A-12)}$$

$$\frac{\partial}{\partial y}[m(p)]=\frac{\partial[m(p)]}{\partial p}\cdot\frac{\partial p}{\partial y}=\left[\frac{2p}{\mu(p)z(p)}\right]\frac{\partial p}{\partial y} \quad \text{..(A-13)}$$

$$\frac{\partial}{\partial z}[m(p)]=\frac{\partial[m(p)]}{\partial p}\cdot\frac{\partial p}{\partial z}=\left[\frac{2p}{\mu(p)z(p)}\right]\frac{\partial p}{\partial z} \quad \text{..(A-14)}$$

thus,

$$\nabla[m(p)]=\left[\frac{2p}{\mu(p)z(p)}\right]\nabla p \quad \text{.....(A-15)}$$

Substitution of equations (A-15) and (A-9) into equation (A-5) reveals

$$\nabla\cdot\left\{\frac{\nabla[m(p)]}{2(\nabla p)}\right\}=\frac{\phi}{k}\frac{pc_0(p)}{z(p)}\frac{\partial p}{\partial t} \quad \text{.....(A-16)}$$

Next, by substituting equation (A-11) into equation (A-16) after solving for $\frac{\partial p}{\partial t}$ it can be found that

$$\nabla\cdot\{\nabla[m(p)]\}=\frac{\phi\mu(p)c_0(p)}{k}\frac{\partial[m(p)]}{\partial t} \quad \text{.....(A-17)}$$

or

$$\nabla^2[m(p)]=\frac{\phi\mu(p)c_0(p)}{k}\frac{\partial[m(p)]}{\partial t} \quad \text{.....(A-18)}$$

Note that equation (A-18) is still non-linear because the diffusivity, $\frac{\phi\mu(p)c_0(p)}{k}$, is a function of a potential. The equation is absent of the assumption of small pressure gradients, and does not require a slow variation of the product $\mu(p)\cdot z(p)$. Also, it is assumed that the permeability, k, in equation (A-18) remains a weak function of pressure. If the permeability's pressure dependence can be regarded as negligible for pressure conditions associated with gas reservoirs (Aronofsky, 1954), then the permeability can be treated as a scalar quantity.

In order to solve equation (A-18), it is necessary to recast the initial and boundary conditions into terms of pseudo-pressure, $m(p)$. An important attribute of equation (A-18) is the gas

mass rate or flux, $\underset{\sim}{v}\rho$, or

$$\underset{\sim}{v}\rho = \frac{\underset{\sim}{q}}{A}\rho = -\frac{Mk}{R_u T}\frac{p}{\mu(p)z(p)}\nabla p \quad \text{.....(A-19)}$$

where, q is the volumetric flow rate, and A is the cross-sectional area. In terms of pseudo-pressure, the gas mass flux of equation (A-19) can be written as

$$\frac{\underset{\sim}{q}}{A}\rho = -\frac{Mk}{2R_u T}\nabla[m(p)] \quad \text{.....(A-20)}$$

The significance of the pseudo-pressure and pseudo-pressure form of the gas mass flux arises through applying the principle superposition theorem (van Everdingen and Hurst, 1949). Superposition allows a linearized system to be used to approximate variable rate flow of real gases in a radial system [Al-Hussainy, *et. al.*, 1966]. Beginning with the "linearized" pseudo-pressure diffusion equation (A-18), a solution is assumed to exist as,

$$m(p) = m(p)[r_D, t_D] \quad \text{.....(A-21)}$$

where,

$t_D = \dfrac{k \cdot t}{\phi\mu(p)c_0(p)r_b^2}$, $r_D = r/r_b$, and r_b are dimensionless time, dimensionless radius (or multiple of the reservoir boundary), and the radius of the reservoir boundary, respectively. Darcy's law expressed in terms of pseudo-pressure, equation (A-20), can be adapted to a gas mass rate as

$$\underset{\sim}{g}(t) = \frac{\underset{\sim}{q}}{A}\rho = -\frac{Mk}{2R_u T}\nabla\{m(p)[r_D, t_D]\} \quad \text{.....(A-22)}$$

or,

$$\underset{\sim}{g}(t) = -\frac{Mk}{2R_u T}\left(r_D \frac{\partial\{m(p)[r_D, t_D]\}}{\partial r_D}\right)_{r_D=1} \quad \text{.....(A-23)}$$

at the reservoir boundary ($r_D = 1$), where $\underset{\sim}{g}(t)$ is the gas mass rate. The cumulative influx of gas mass is then the integral of (A-23) or

$$\underset{\sim}{G}(t) = \int_0^t \underset{\sim}{g}(t) = -\frac{Mk}{2R_u T}\cdot\frac{\phi\mu(p)c_0(p)r_b^2}{k}\cdot\int_0^{t_D}\left(r_D \frac{\partial\{m(p)[r_D, t_D]\}}{\partial r_D}\right)_{r_D=1} dt_D$$
.....(A-24)

$$\underset{\sim}{G}(t) = \int_0^t \underset{\sim}{g}(t)dt = -\frac{Mk}{2R_u T}\cdot\frac{\phi\mu(p)c_0(p)r_b^2}{k}\cdot Q(t_D)$$
.....(A-25)

where,

$$Q(t_D) = \int_0^{t_D}\left(\frac{\partial\{m(p)[r_D, t_D]\}}{\partial r_D}\right)_{r_D=1} dt_D \quad \text{.....(A-26)}$$

Using the general solution for the cumulative gas mass influx, equation (A-26), expressed in integration of dimensionless time, t_D, of the pseudo-pressure gradient at r_D = 1 for a pseudo-pressure drop of 1.0 Pa/s (or 1.0 Atmospheres/s), the cumulative influx into the wellbore can be computed from equation (A-25). Furthermore, for any pseudo-pressure drop, $\Delta\{m(p)[r_D, t_D]\}$, equation (A-27) expresses the cumulative gas mass influx as

$$\underset{\sim}{G}(t) = -\frac{M}{2R_u T}\cdot\phi\mu(p)c_0(p)r_b^2\cdot\Delta\{m(p)[r_D, t_D]\}\cdot Q(t_D)$$
.....(A-27)

per unit reservoir thickness. Equation (A-27) can be recast into as

$$\underset{\sim}{G}(t) = \Delta\{m(p)[r_D, t_D]\}\cdot I(t_D) \quad \text{.....(A-28)}$$

where,

$$I(t_D) = -\frac{M}{2R_u T}\cdot\phi\mu(p)c_0(p)r_b^2\cdot Q(t_D) \quad \text{.....(A-29)}$$

is the influence function.

The "linearity" of the pseudo-pressure form diffusion equation (A-18) allows the application of theorem of superposition to describe a sequence of constant terminal pressures (or pseudo-pressures), such that it reproduces the pseudo-pressure history of the wellbore boundary, $r_D = 1$.

Shown in Figure 18 is the pseudo-pressure history reproduced by a sequence of constant terminal pseudo-pressures. As noted by Van Everdingen and Hurst (1949), the constant terminal pressure condition is a scenario where at zero time there exists a homogeneous initial pressure at all radial positions and when the wellbore is opened, the pressure at the boundary of the reservoir drops to a "terminal" pressure. Therefore applying equation (A-29), the cumulative gas mass produced in time t_D by pseudo-pressure drop, $\Delta[m(p)]_0$, operative since zero time, can be expressed as

$$\underset{\sim}{G}(t) = \Delta[m(p)]_0 \cdot I(t_D) \quad \text{.....(A-30)}$$

Next, consider the pseudo-pressure drop, $\Delta[m(p)]_1$, which occurs at time t_1, and then treat this as a separate entity, but take cognizance of its time inception t_1. Then the cumulative gas mass produced during this increment in pseudo-pressure drop is

$$\underset{\sim}{G}(t) = \Delta[m(p)]_1 \cdot I(t_D - t_1) \quad \text{.....(A-31)}$$

Therefore by **superimposing** all these effects of pseudo-pressure changes, the total gas mass influx in time t can be expresses as

$$\underset{\sim}{G}(t) = \Delta[m(p)]_0 \cdot I(t_D) + \Delta[m(p)]_1 \cdot I(t_D - t_1) + \Delta[m(p)]_2 \cdot I(t_D - t_2) + \Delta[m(p)]_3 \cdot I(t_D - t_3) + \ldots$$

.....(A-32)

when $t > t_3$.

To reproduce the smooth curve relationship of Figure 9, these pseudo-pressure plateaus can be taken as infinitesimally small, which then result the convolution integral

$$\underset{\sim}{G}(t) = \int_0^{t_D} \frac{\partial\{m(p)][r_D, t_D]\}}{\partial t'} I(t_D - t')dt' \quad \text{.....(A-33)}$$

or

$$\underset{\sim}{G}(t) = \int_0^{t_D} \Delta\{m(p)][r_D, t_D]\} \cdot I(t_D - t')dt' \quad \text{.....(A-34)}$$

A numerical approximation form equation (A-34) may be written as

$$\underset{\sim}{G}(t_n) = \sum_{j=1}^{n} [m(p)_{j-1} - m(p)_j] \cdot I(t_n - t_{j-1}) \quad \text{.....(A-35)}$$

A linear system describing use of the influence function is shown schematically in Figure 5.

The Influence function can be generated from an approximate mathematical solution (*e.g.*, TOUGH28W finite difference code) to the transient radial flow equation:

$$\frac{\partial^2 p^2}{\partial r^2} + \frac{1}{r}\frac{\partial p^2}{\partial r} = \frac{\phi\mu(p)c_0(p)}{k}\frac{\partial p^2}{\partial t} \quad \text{.....(A-36)}$$

where $c_0(p)$ is the reciprocal of pressure for an Ideal gas, or $c_0(p) = p^{-1}$. Equation (A-36) is the radial symmetric equivalent form of equation (A-7). Again, transforming the transient radial flow equation into pseudo-pressure form, it follows that

$$\frac{\partial^2[m(p)]}{\partial r^2} + \frac{1}{r}\frac{\partial[m(p)]}{\partial r} = \frac{\phi\mu(p)c_0(p)}{k}\frac{\partial[m(p)]}{\partial t} \quad \text{.....(A-37)}$$

Similarly, equation (A-37) is the radial symmetric equivalent form of equation (A-18). Typically the reservoir simulators do not solve the pseudo-pressure and cumulative gas mass influx directly, and are generally designed to use numerical techniques to solve the transient radial symmetric gas flow problem, equation (A-36). However, from the reservoir simulator solutions, both the pressure and gas volume rate histories can be solved. Knowledge of equations (A-10) and (A-20) can then be used to determine both the pseudo-pressure and the gas mass flux histories. Thus using results from the reservoir numerical model (*e.g.*, TOUGH28W), the Influence function can readily be assembled as the cumulative gas mass influx divided by the pseudo-pressure drop (or delta pseudo-pressure)

$$I \equiv \frac{\text{Cumulative Gas Mass Influx}}{\text{Pseudo} - \text{Pressure Drop}} \quad \text{.....(A-38)}$$

Next the Influence function can be used to determine the cumulative gas mass influx in a wellbore hydraulics simulator (*e.g.*, KICK, COMBOF, etc.) by specifying an input pseudo-pressure drop into the linearized system. This now allows the cumulative gas mass influx to be determined without direct coupling to a numerical reservoir calculation code (*e.g.*, TOUGH28W, etc.).

Table 1-Base Case Input Parameter Values for COMBOF Sensitivity Analysis		
Parameter	**Units**	**Value**
Total depth	m	654.10
Collar diameter	m	0.2032
Collar length	m	182.88
Drill pipe diameter	m	0.1143
Drill pipe length	m	471.22
Drilled diameter	m	0.31115
Spalled particle diameter	Microns	300
Particle specific gravity	n/a	2.65
Particle density	kg/m^3	2650
Waste room permeability	m^2	1.7x10-13
Waste room porosity	m^3/m^3	0.6
Waste room initial pressure	MPa	14.8
Drilling mud density	kg/m^3	1230
Drilling mud viscosity	CPoise	8.0
Temperature gradient	°F/ft	0.0225
Maximum allowed solids-to-gas volume flow ratio	%	4.00
Gas specific gravity	n/a	0.06959 (equiv. to H_2)

Table 2-Drilling Mud Density Used in COMBOF Sensitivity Analysis		
Parameter	**Units**	**Values**
Drilling mud density	kg/m^3	980.0 to 1277.5 (18 intervals)
All others	n/a	Same as Base Case

Table 3-Drilling Mud Viscosity Used in COMBOF Sensitivity Analysis		
Parameter	**Units**	**Values**
Drilling mud viscosity	cPoise	1.0 to 100.0 (19 intervals)
All others	n/a	Same as Base Case

Table 4-Solids-to-Gas Volume Flow ratio Used in COMBOF Sensitivity Analysis		
Parameter	**Units**	**Values**
Maximum allowed solids-to-gas volume flow ratio	%	1.00 to 6.00 (by 0.25 increments)
All others	n/a	Same as Base Case

Table 5-Rate of Penetration Drilling Sequence Used in KICK Sensitivity Analysis

t-t_{stab} [min]	Rate of Penetration [ft/hr]	Pumping Rate [gpm]	Drill Bit Depth (DBD) [ft, in]	ΔDBD [in]	Depth into Gas Zone [in]	Time Gas Zone Exposed [sec]
0	50	300	2145' 0"	0"	0	0
1	50	300	2145' 10"	10"	0	0
4	50	400	2148' 4"	40"	0	0
6	50	400	2150' 0"	60"	0	0
7	0	400	2150' 10"	70"	10"	60
7.85*	0	400	2150' 10"	70"	10"	111

Table 6-Base Case Input Parameters Used in KICK sensitivity analysis

Parameter	Units	Value
Total depth	m	654.10
Collar diameter	m	0.2032
Collar length	m	182.88
Drill pipe diameter	m	0.1143
Drill pipe length	m	471.22
Drilled diameter	m	0.31115
Drill cuttings specific gravity	n/a	2.5
Gas Zone Permeability	m^2	$1.7x10^{-13}$
(Gas Zone Permeability)	(mDarcy)	(172.26)
Gas zone pressure	MPa	14.79
(Gas zone pressure)	(equiv. ppg)	(19.00)
Drilling mud density	kg/m^3	1079.52
(Drilling mud density)	(ppg)	(9.00)
Drilling mud plastic viscosity	cPoise	4.0
Gas slip velocity	m/sec	0.244
(Gas slip velocity)	(ft/sec)	(0.80)
Mud pumping rate {after 60 seconds of drilling}	m^3/s	1.135
(Mud pumping rate {after 60 seconds of drilling})	(gpm)	(300)
Mud pumping rate {after 240 seconds of drilling}	m^3/s	1.514
(Mud pumping rate {after 240 seconds of drilling})	(gpm)	(400)
Temperature gradient	°F/ft	0.01
Gas specific gravity	n/a	0.6

Table 7-Drilling Mud Density Used in KICK Sensitivity Analysis

Parameter	Units	Values
Drilling mud density	kg/m^3	1000.0, 1079.5, 1230.0
(Drilling mud density)	(ppg)	(8.3370, 9.0000, 10.2545)
All others	n/a	Same as Base Case

Table 8-Gas Slip Velocity Ratio Used in KICK Sensitivity Analysis

Parameter	Units	Values
Gas slip velocity	M/sec	0.000, 0.244, 0.488
(Gas slip velocity)	(ft/sec)	(0.000, 0.800, 1.600)
All others	N/a	Same as Base Case

Table 9-Permeability Used in KICK Sensitivity Analysis		
Parameter	**Units**	**Values**
Gas Zone Permeability	m^2	5×10^{-14}, 1.7×10^{-13}, 5×10^{-13}
(Gas Zone Permeability)	(mDarcy)	(50.65, 172.26, 500.065)
All others	n/a	Same as Base Case

Table 10-Solids-to-Gas Volume Flow Ratios Used in KICK Calculations with Spalling Mechanism		
Parameter	**Units**	**Values**
Solids-to-Gas volume flow ratio	%	1, 2, 3, 4, 5, 6, 7, 10
All others	n/a	Same as Base Case

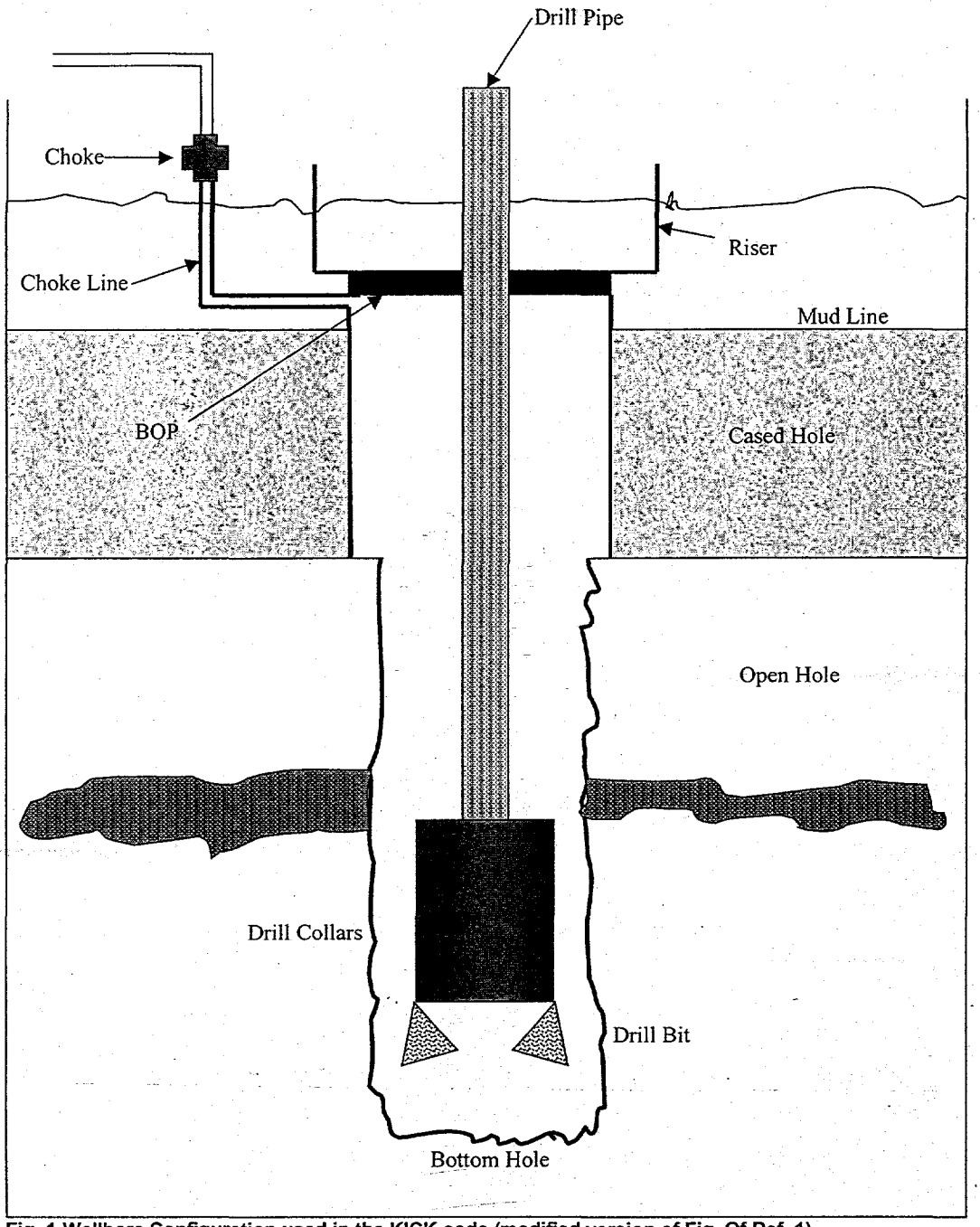

Fig. 1-Wellbore Configuration used in the KICK code (modified version of Fig. Of Ref. 1)

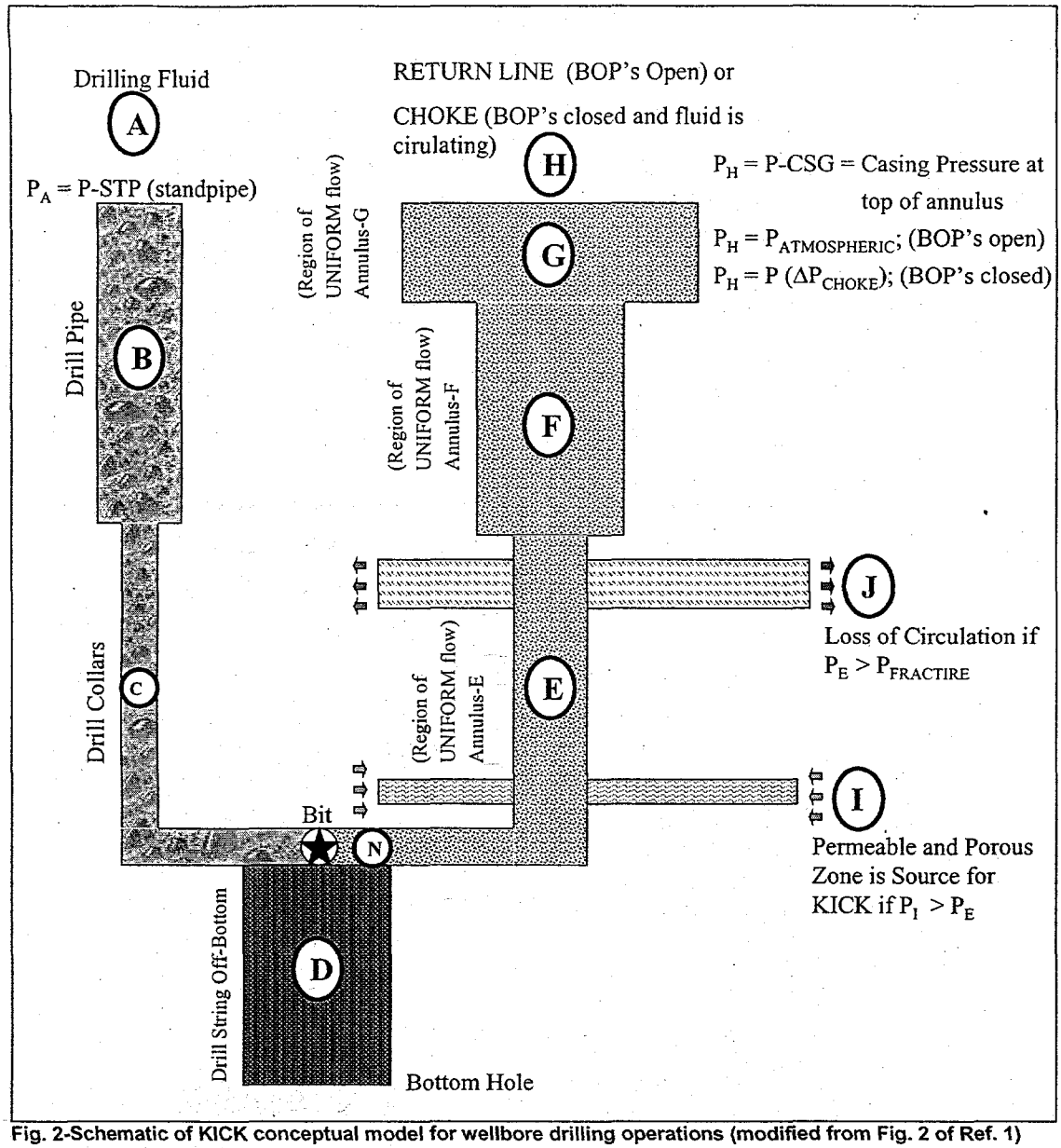

Fig. 2-Schematic of KICK conceptual model for wellbore drilling operations (modified from Fig. 2 of Ref. 1)

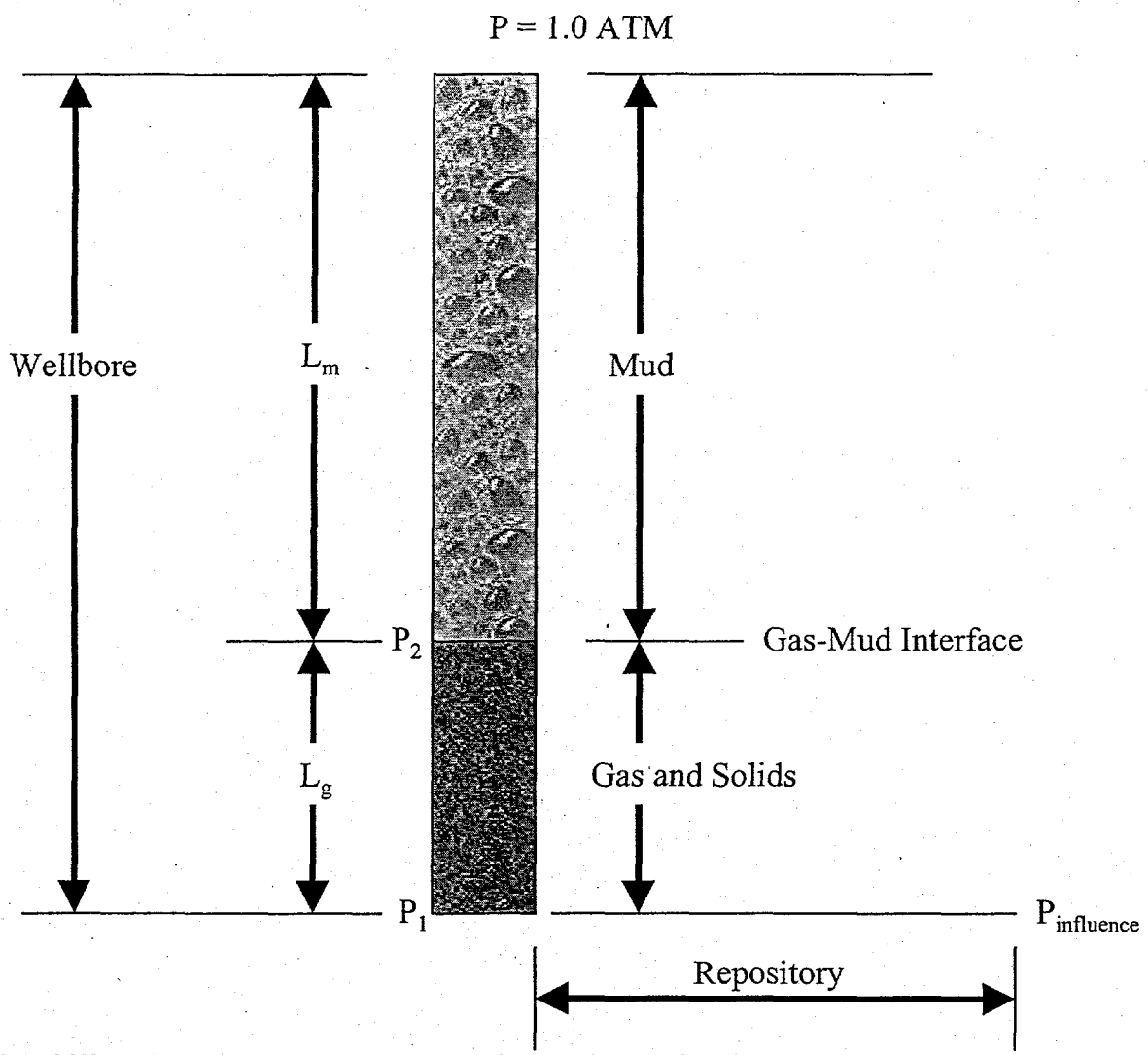

Fig. 3-COMBOF Conceptual model for single slug of mud and single slug of gas and solids (Modified from Fig. 2-1 of Ref. 3)

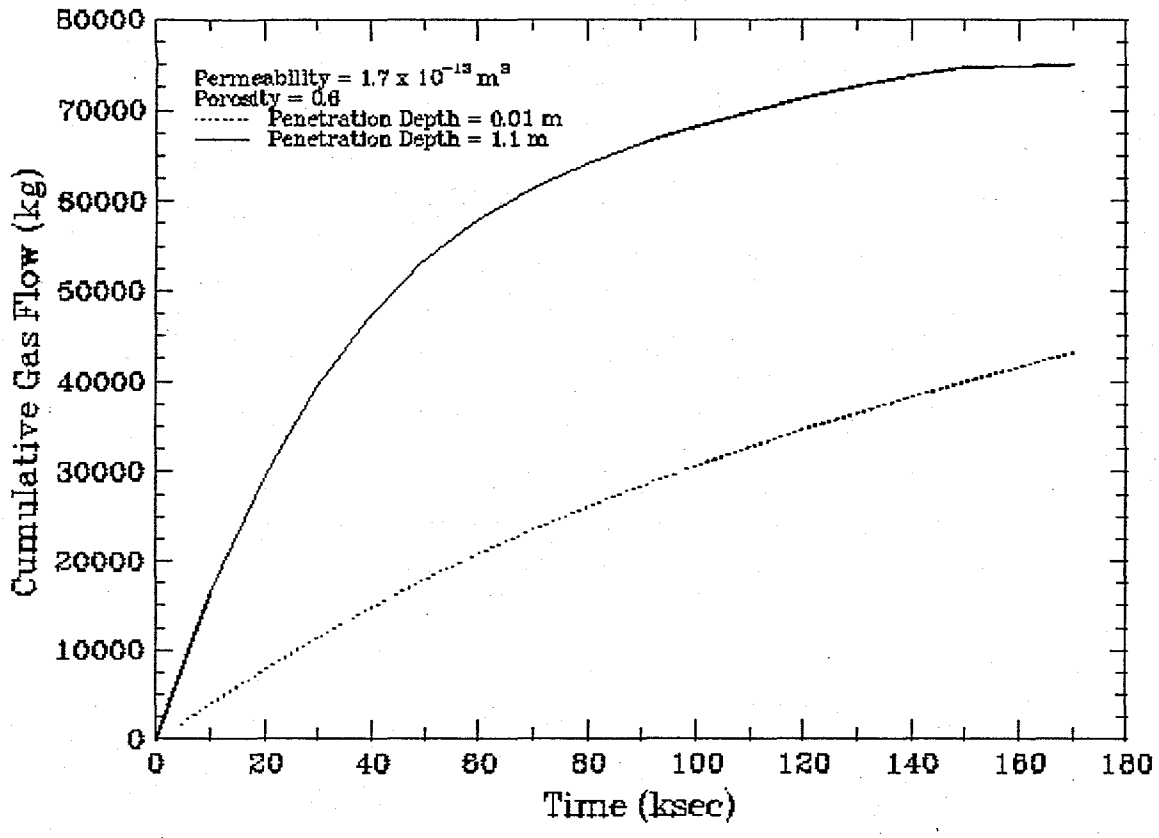

Fig. 4-Cumulative Gas Production from TOUGH28W Calculations for Two Different WIPP Waste Panel Penetration Depths

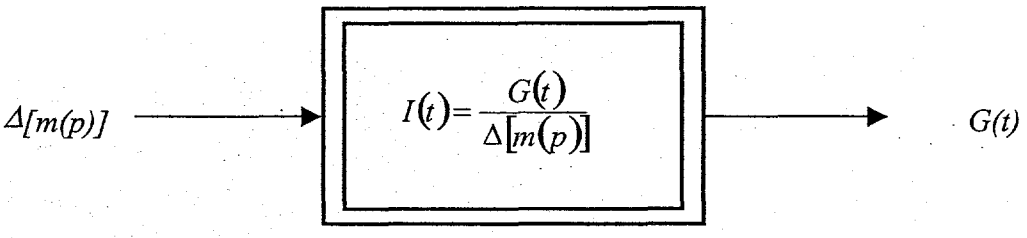

Fig. 5-Linear System Used for Determining Cumulative Gas Mass Influx

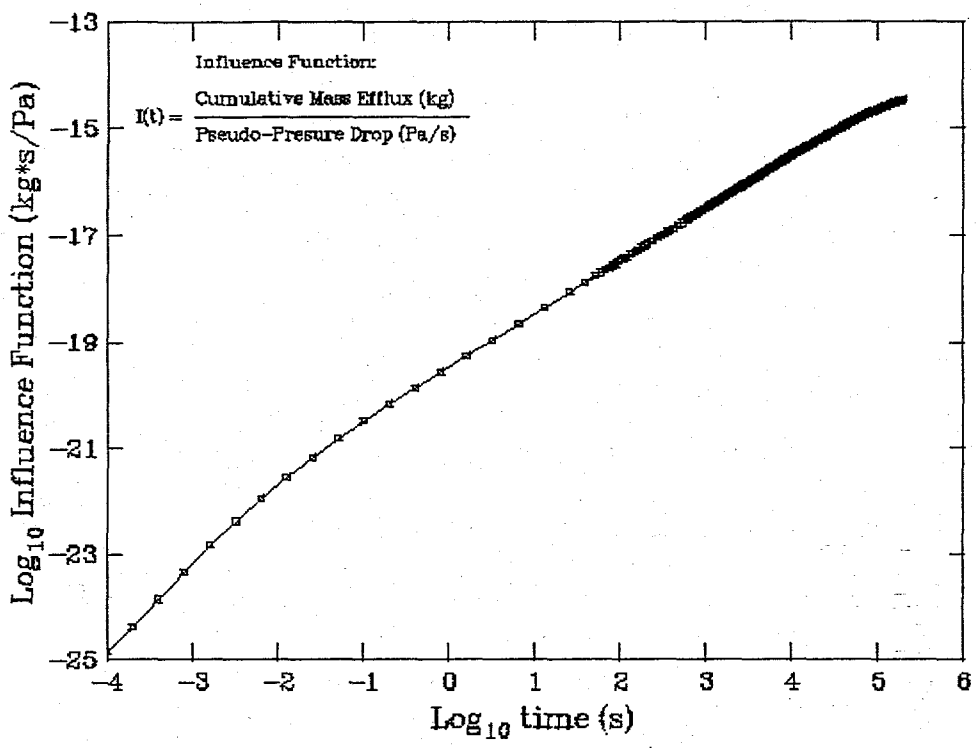

Fig. 6-Influence Function vs. Time Used in all wellbore hydraulics simulator Calculations

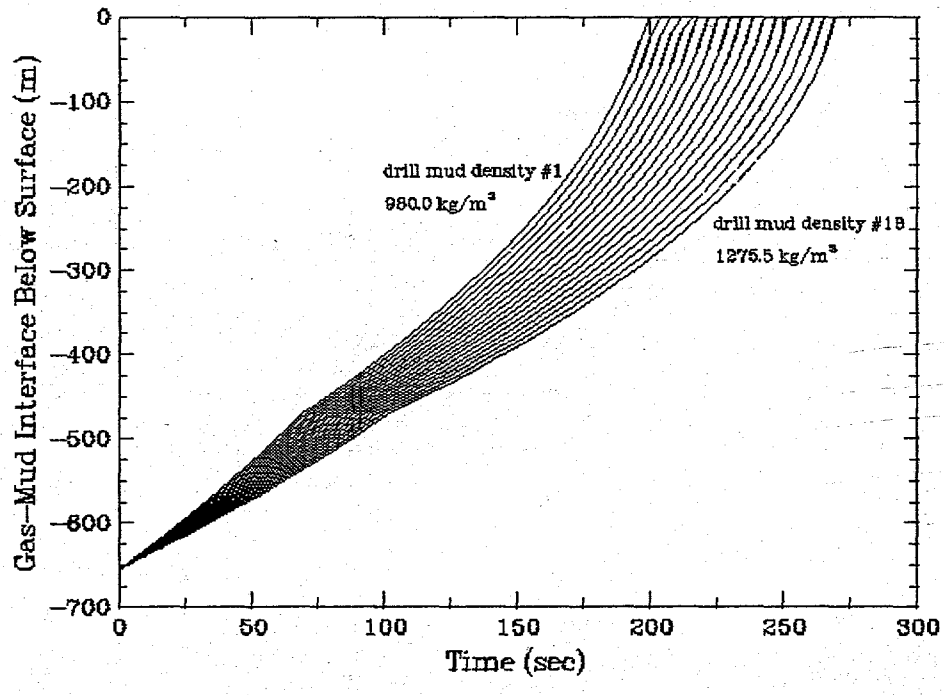

Fig. 7-Psuedo-Pressure vs. Pressure Used in all wellbore hydraulics calculations

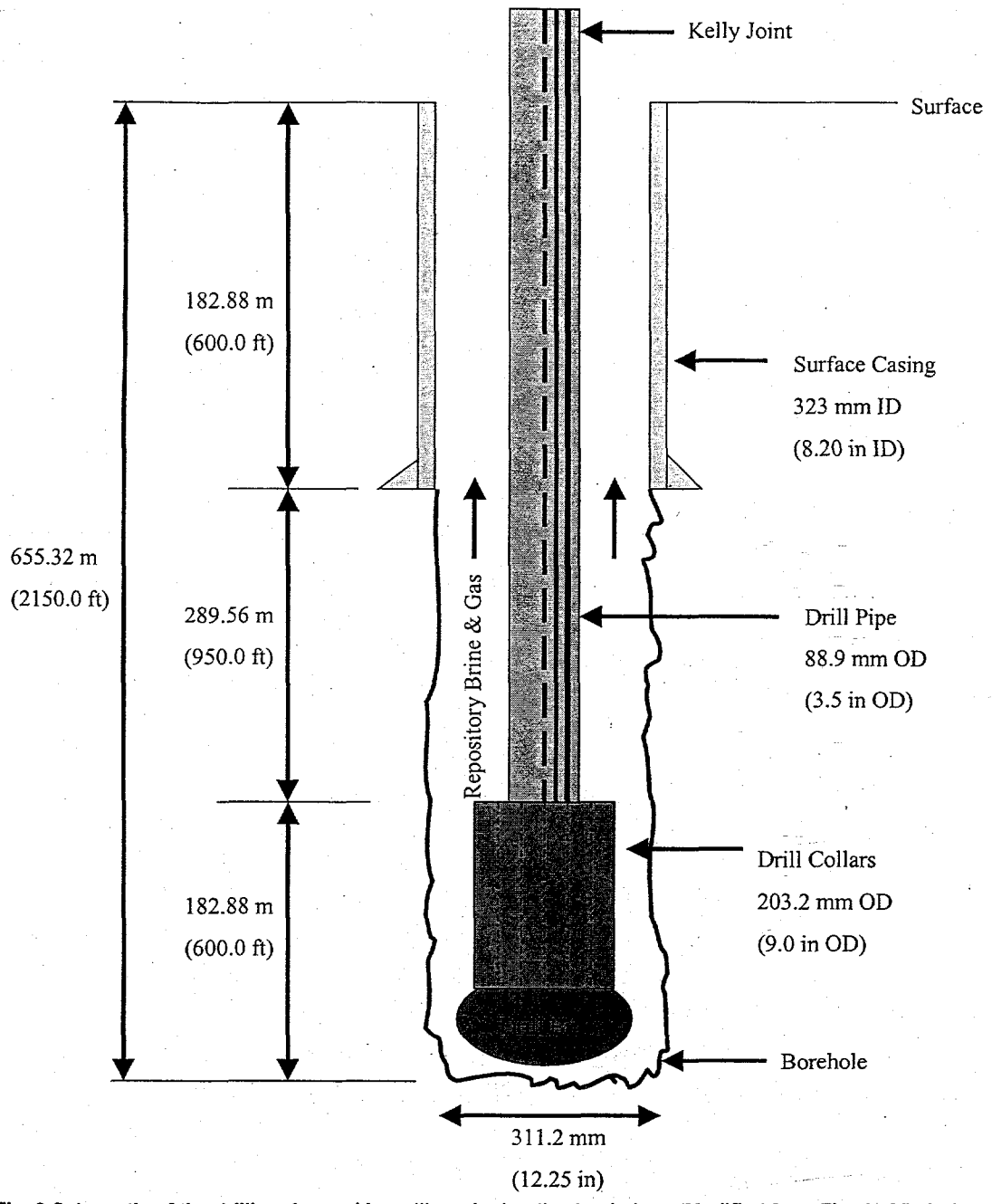

Fig. 8-Schematic of the drilling rig used in wellbore hydraulic simulations (Modified from Fig. 4 of Ref. 5)

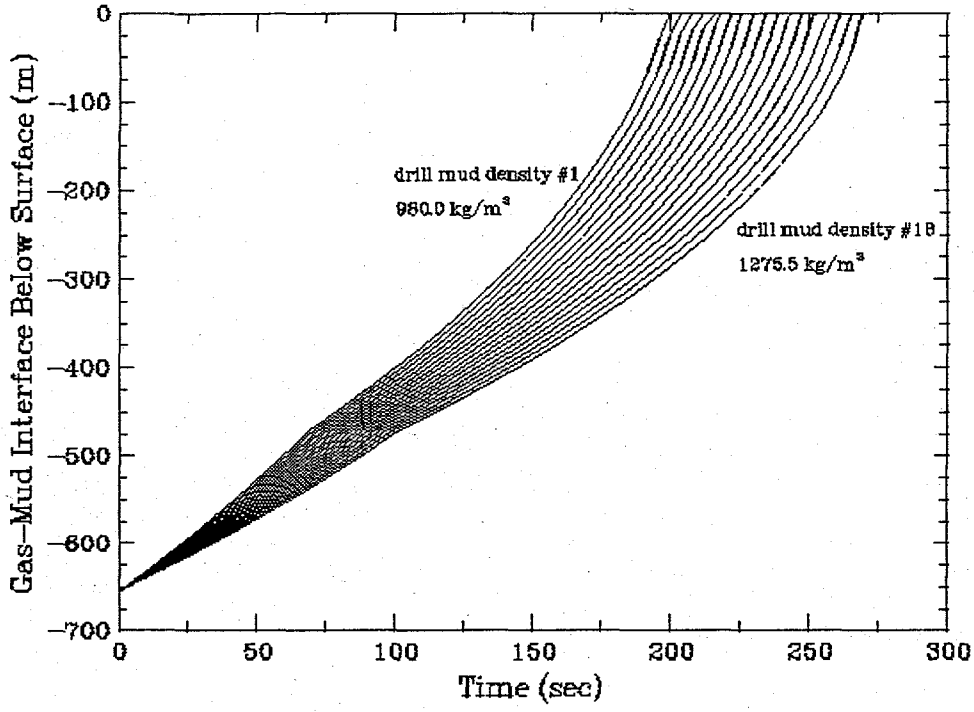

Fig. 9-COMBOF calculation, varying mud density, for GMI elevation response history

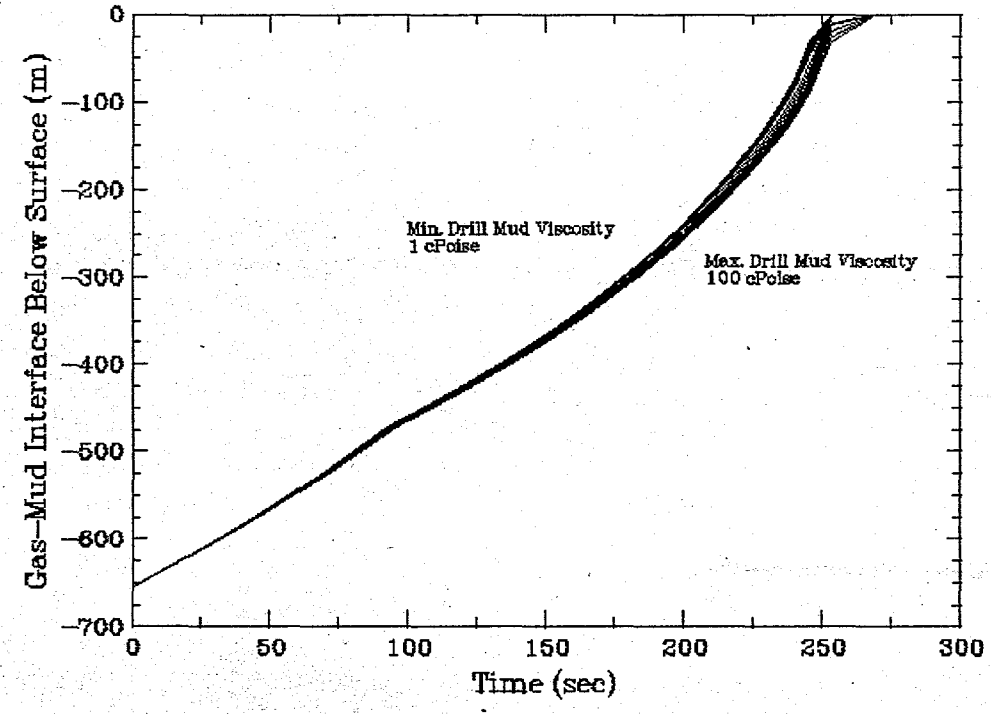

Fig. 10-COMBOF calculation, varying mud density, for GMI elevation response history

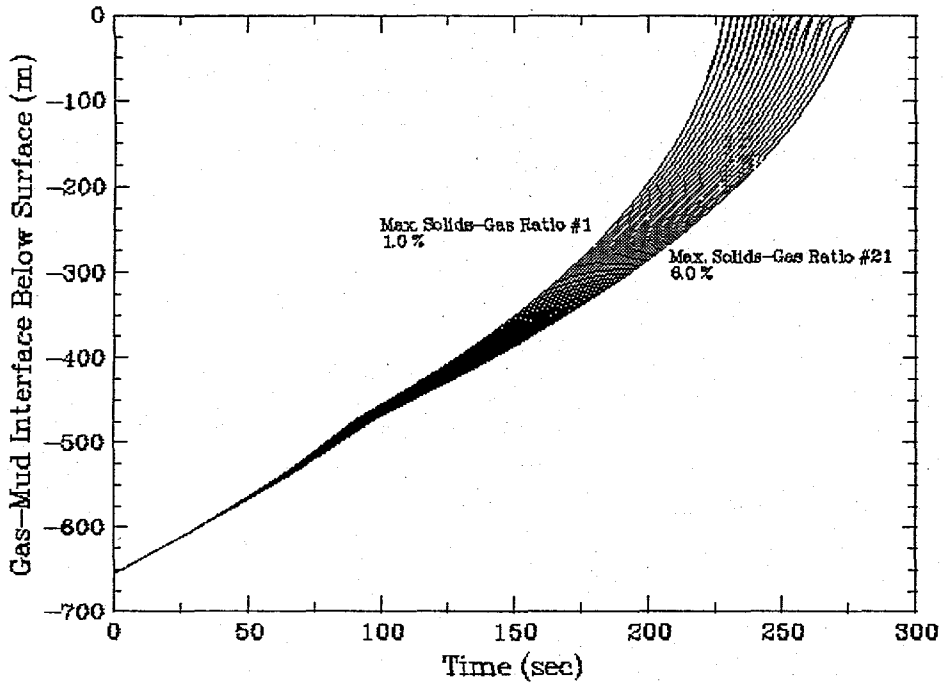

Fig. 11-COMBOF calculation, varying drilling mud viscosity, for GMI elevation response history

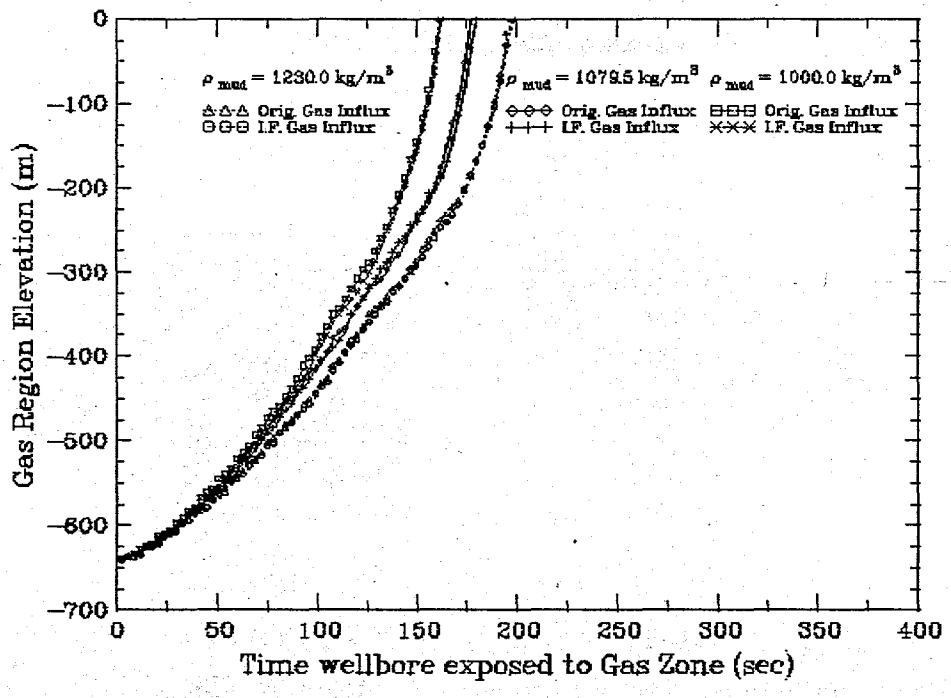

Fig. 12-KICK calculation, varying drilling mud density, for GMI-elevation response history

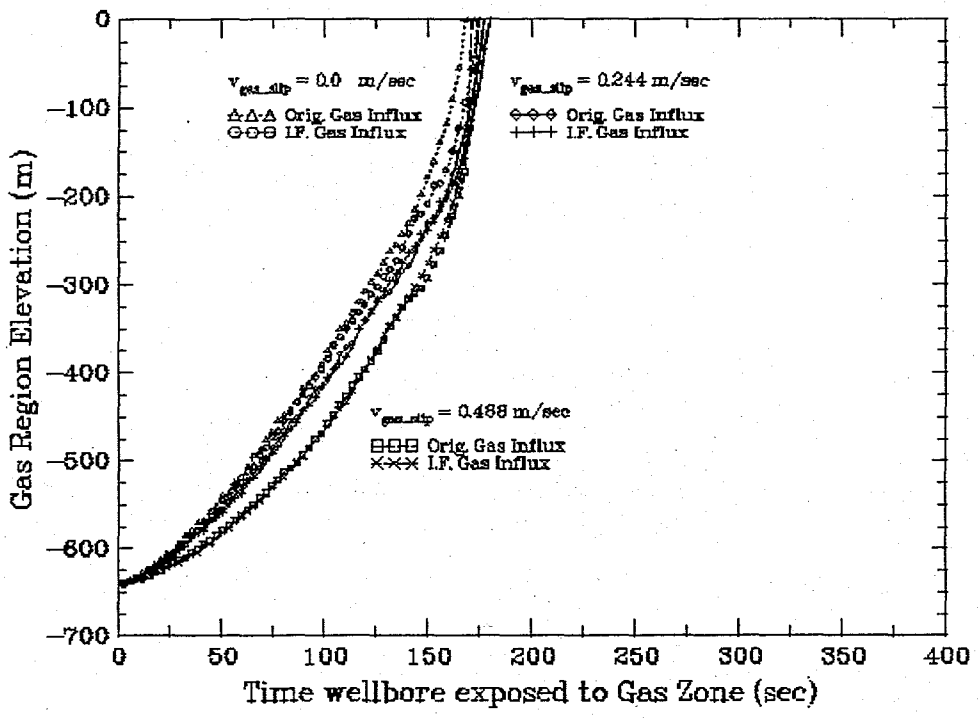

Fig. 13-KICK calculation, varying gas-slip velocity ratio, for GMI-elevation response history

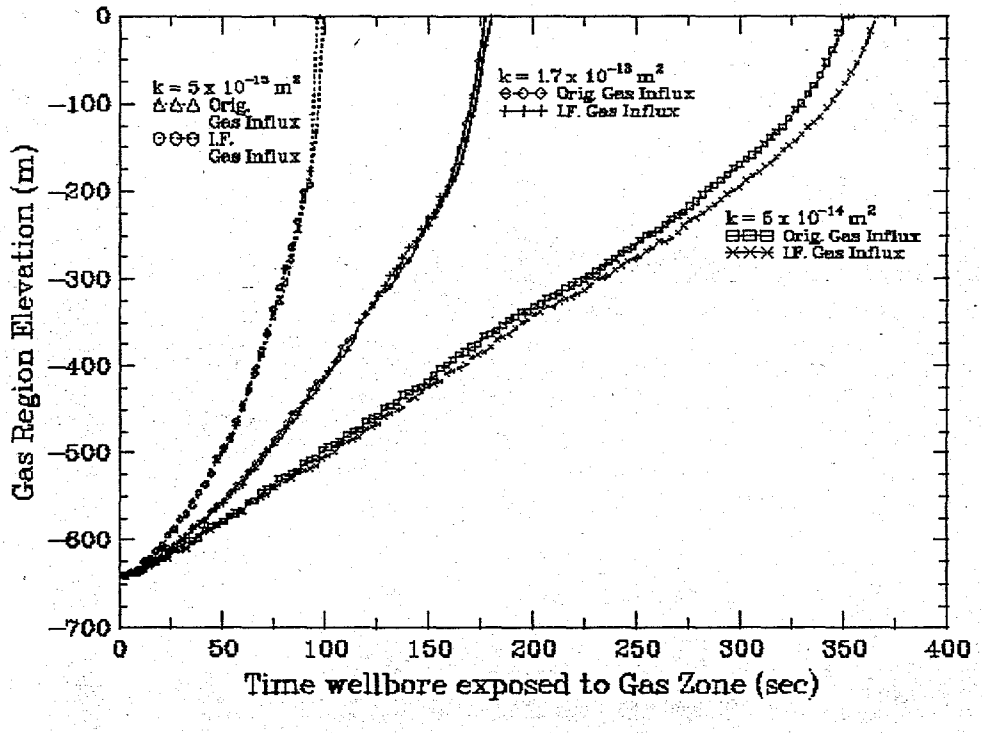

Fig. 14-KICK calculation, varying gas zone (i.e., repository) permeability, GMI-elevation response history

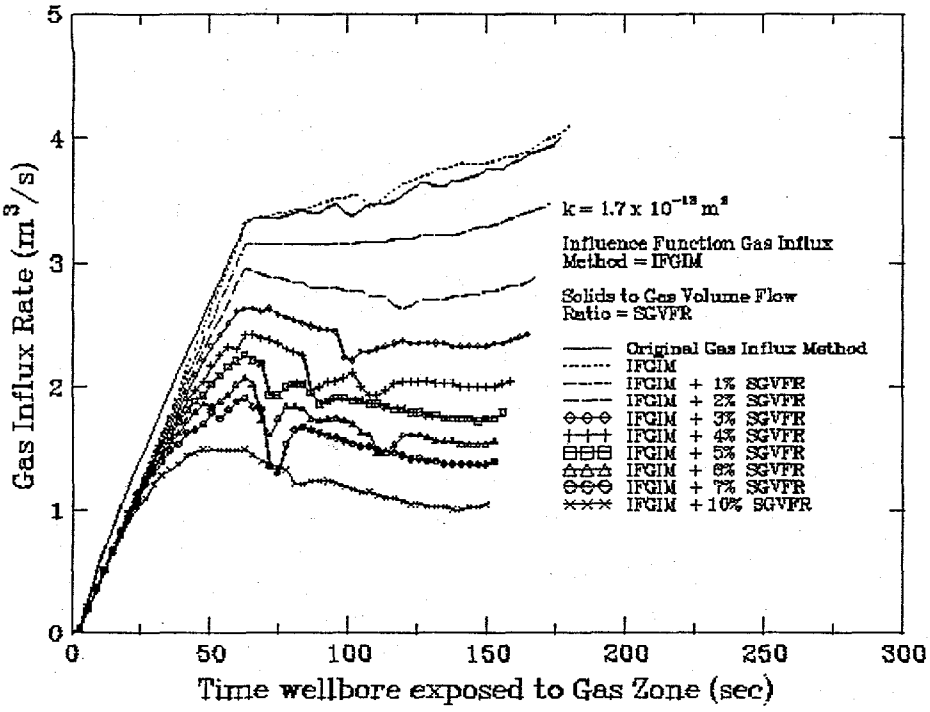

Fig. 15-KICK calculation, added Influence Function gas influx and spalling effects, Gas elevation vs. time

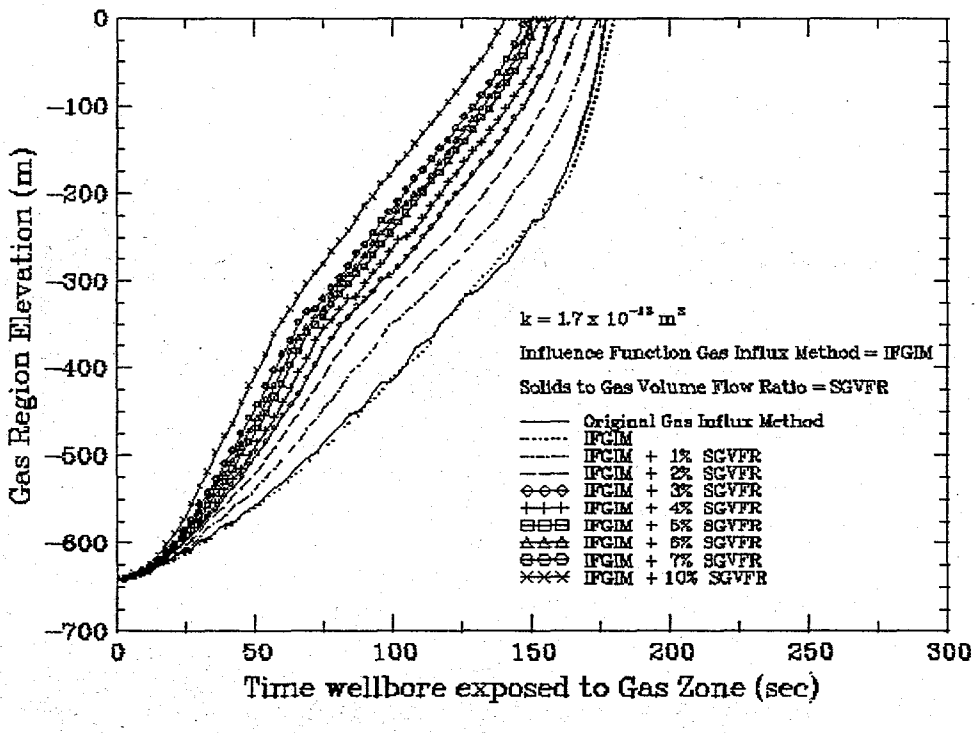

Fig. 16-KICK calculation, added Influence Function gas influx and spalling effects, Gas Influx Volume Rate vs. time

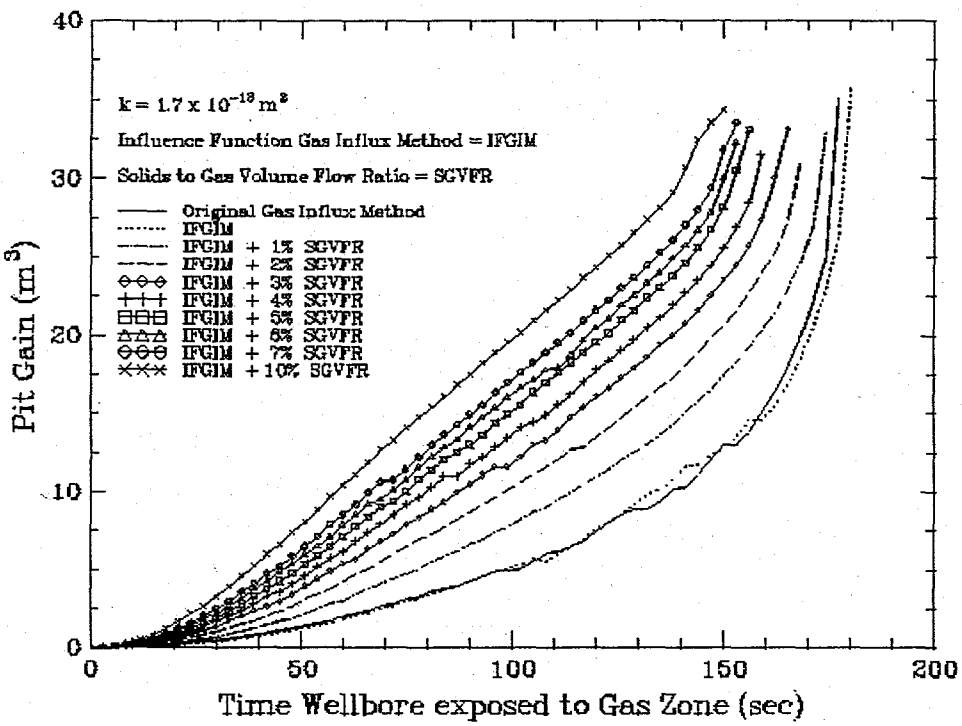

Fig. 17-KICK calculation, added Influence Function gas influx and spalling effects, Pit Gain vs. time

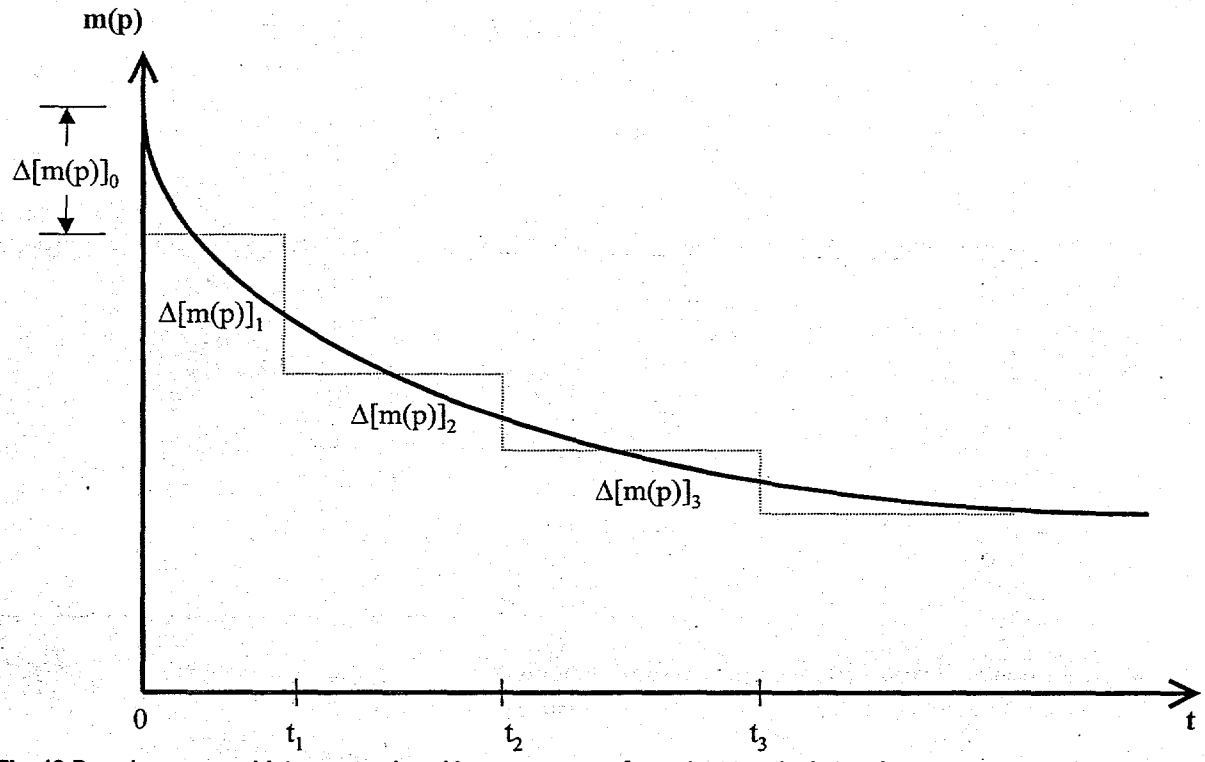

Fig. 18-Psuedo-pressure history reproduced by a sequence of constant terminal pseudo-pressures